

# Categories of Quantum Photoinitiators

Subjects: Polymer Science

Contributor: shubhangi shukla

The use of novel photoinitiators (PIs) for free-radical polymerization has attracted significant attention from the scientific community. Quantum PIs, quantum-confined nanoscale crystals with semiconductor properties, have received interest for use in photopolymerization, due to their precisely tunable properties as a function of structural and surface engineering.

Keywords: quantum photoinitiators ; upconverting nanoparticles ; quantum confinement effect ; semiconductor nanocrystals

## 1. Introduction

Current advancements in synthetic procedures have led to the development of a variety of quantum PIs with characteristic photoinitiating properties [1][2][3][4][5][6][7]. The surface moieties introduced in the course of nanocrystal synthesis facilitate control over skeletal arrangements, dispersibility, and reactivity at the molecular level [8][9][10][11][12][13][14][15][16][17]. Postsynthetic surface modifications enable the dispersal and stabilization of nanocrystals PIs in formulations for many applications [2][3][4][5][6][7][11][12][13][14][15][16][17][18][19][20].

Several classes of quantum PIs have been developed and evaluated for polymerization, with various absorption and excitation wavelength windows [15][16][17][18][19][20]. The mode of action of most of the quantum PIs is generally similar to type I radical initiators, with highly conjugated aromatic moieties; others mimic the activity of type II initiators [2][3][4][5][6][7]. Loir et al. indicated that two pathways exist for initiation in quantum PIs, which involve surface mediated hole transfer (**Figure 1**) [7]. Typical quantum PIs can be classified as semiconductor nanoparticles (NPs), such as  $\text{TiO}_2$ ,  $\text{ZnO}$ , and  $\text{CdS}$  NPs [10][11][2][3][4][5][6][7][11][12][13][14][15][16]; hybrid photoinitiators, including composites of metal nanoparticles (MNPs)/silanized metal (organic PIs, MNPs), fluorescent dyes, oligomeric silsesquioxane, and parent PIs, [17] semiconductor NPs (metal/graphene oxide) [18][19][20][21][22][23], and organometallic nanoparticles; panchromatic photoinitiators, namely upconverting nanoparticles (UCNPs) [24][25][26][27][28][29][30][31][32][33][34] and plasmonic nanoparticle composites (e.g.,  $\text{Ag@SiO}_2\text{@UC@BFO-Au}$  core@triple-shell); near-infrared photoinitiators, such as luminescent lanthanides (e.g.,  $\text{Ln}^{3+}$ ,  $\text{Yb}^{3+}$ ,  $\text{Er}^{3+}$ , and  $\text{Ho}^{3+}$ ) and doped nanomaterials in a crystalline host lattice ( $\text{NaYF}_4$ ); [31] magnetic nanoparticles, such as  $\text{Fe}_2\text{O}_3$ ; and metal core-shell nanoparticles (e.g.,  $\text{Ag@AgCl}$  nanocubes) [35][36]. **Figure 2** describes the polymerization of acrylic acid sodium (AAS) using the  $\text{Ag@SiO}_2\text{@UC@BFO-Au}$  photoinitiator.

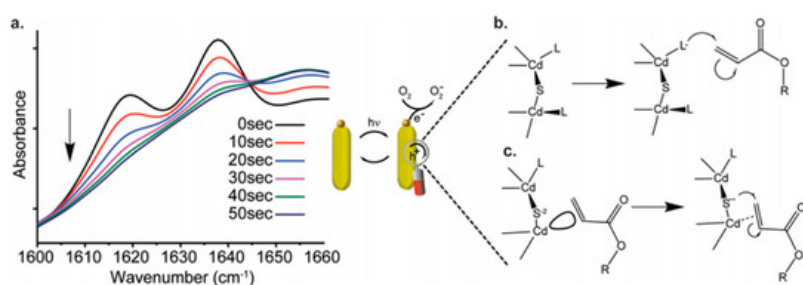


**Figure 1.** Insights into the mechanism. (a) FTIR spectra of the polymerization process of hydroxyethyl acrylate (HEA) using  $\text{CdS-S}^{2-}$  in the presence of water. The C=C doublet at  $1619\text{ cm}^{-1}$  and  $1637\text{ cm}^{-1}$  disappears with illumination time. (b) Proposed Mechanism 1: the initiation is carried out by hole transfer from the semiconductor to the monomers via surface coating mediation. (c) Proposed Mechanism 2: the double bond is coordinated by the cation, followed by a hole transfer from the anion-localized state [7].

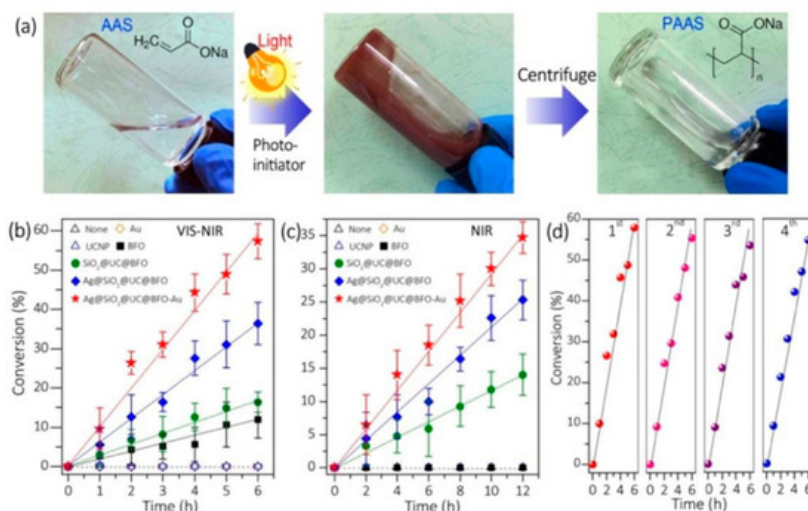


**Figure 2.** (a) Pictures of acrylic acid sodium (AAS) aqueous solution without NP photo-initiator (left), after polymerization reaction before (middle), and after (right) removal of  $\text{Ag@SiO}_2@\text{UC@BFO-Au}$  initiator. Conversion of AAS using different NPs as initiators under white light (b) and near infrared (NIR) light (c) (the lines are to guide the eyes). (d) Repeated runs for the polymerization using  $\text{Ag@SiO}_2@\text{UC@BFO-Au}$  under VIS light [31].

## 2. Categories of Quantum Photoinitiators

### 2.1. Semiconductor QPIs

Quantum photoinitiators based on semiconductor nanocrystals are considered a viable alternative to traditional organic photoinitiators with low molecular weights. Semiconductor nanocrystals have attracted attention due to their capacity to function as photocatalysts for many types of chemical reactions; these materials offer unique advantages, such as efficient light-harvesting activity, tunable properties, and large surface area-to-volume ratios [9]. These nanocrystals exhibit quantum confinement effects; the properties of these materials may be modified by synthetic control over nanocrystal size, shape, and composition [9].

Semiconductor quantum dots (QD) are solution-dispersible nanocrystals, which have found use as photocatalysts for light-induced polymerization. QDs exhibit strong absorption in the UV-visible range, with large extinction coefficients ( $\epsilon > 10^5 \text{ M}^{-1} \text{ cm}^{-1}$ ) [14], large specific surface area values that allow for the interaction with multiple substrates, and higher photostability than organic-based photocatalysts and transition metal complexes [14]. Semiconductor suspensions were first used for photopolymerization by Kuriacose et al.; ZnO powders were used for photopolymerization of methyl methacrylate (MMA) in water [8]. The effect of the oxygen level on polymerization was investigated; higher amounts of oxygen were associated with a lower molecular weight and a larger number of chains. On the other hand, too much oxygen in the solution suppressed the propagation step; this phenomenon was reported to be a common limitation for polymerization initiated by oxidative anionic species-releasing photoinitiators.

### 2.2. Carbon-Based QPIs

Various efforts have been made to obtain carbon dots (CDs) from naturally occurring materials [37][38][39]. Owing to their straightforward preparation, capability for preparation from sustainable raw materials, and ultrastable photoluminescence, photoluminescent CDs have been utilized in bioimaging, optoelectronics, photocatalysis, and photopolymerization [37].

For example, Kiskan et al. used mesoporous graphitic carbon nitride ( $\text{mpg-C}_3\text{N}_4$ ) alongside tertiary amine co-initiators for visible-light-induced free radical polymerization via a hybrid type II initiator approach [37]. This approach involved generating radical initiators by scavenging holes using amines and hydrogen abstraction. The surface area of the carbon nitride powder and the type of amines were shown to affect the photoinitiation efficiency associated with this approach (e.g., more basic amines enhance the efficiency of the approach).

### 2.3. Graphene-Based QPIs

Graphene sheets are known to exhibit extraordinary electronic transport properties, thermal conductivity, mechanical stiffness, and fracture strength [19]. Graphene was physically dispersed into polymer precursors; polymerization of this material was performed under UV illumination. Rapid transformation of a liquid monomer into a solid film with tailored mechanical properties and physical-chemical properties was demonstrated [22]. Recent studies on graphene derivatives have demonstrated the ability of graphene oxide (GO) to initiate radical polymerization of acrylic monomers on thermal or

photochemical reduction [18][19][20][21][22]. The findings have opened new routes to produce polymer-GO hybrid composites with pH-responsive behavior, high electrical conductivity, improved thermal stability, and exceptional absorbency. Polymers such as polyvinylpyrrolidone or polyvinyl acetate grafted with graphene oxide exhibit good solubility in organic solvents and may be utilized for this approach [18][19][20][21][22][23].

Andryushina et al. investigated the photopolymerization using UV-visible light of acrylamide in aqueous solutions that included colloidal graphene oxide [20]. Graphene oxide was first observed as a water-soluble photoinitiator for polymerizing acrylamide. It was observed that the efficiency of polymerization was associated with the activity of photoexcited oxygen functionalities of GO; the higher the density of these groups, the greater the growth of the polymer.

Feng et al. demonstrated the fabrication of superhydrophobic surfaces from a formulation containing the I-907 free-radical photoinitiator, thiol-coupled graphene nanosheets, ethoxylated bisphenol A diacrylate, and 2-(perfluorooctyl) ethyl acrylate, which were prepared via a photopolymerization process [21]. Light-induced cross-linking between the reactive graphene nanosheets and the reactive monomers led to the formation of a robust self-wrinkling surface morphology, due to a UV curing process-generated inner tension within the composite (**Figure 3**). The presence of residual fluorine groups enabled strong cohesive forces, leading to the growth of surfaces with oleophobicity, as well as superhydrophobicity. Using this approach, a coating with a nonstick appearance was obtained. The superhydrophobic character of the material was maintained at extreme pH conditions (1–12); the material was able to withstand a prolonged UV-irradiation time of 120 h. This approach may enable the large-scale fabrication of surfaces with superhydrophobic properties [21].

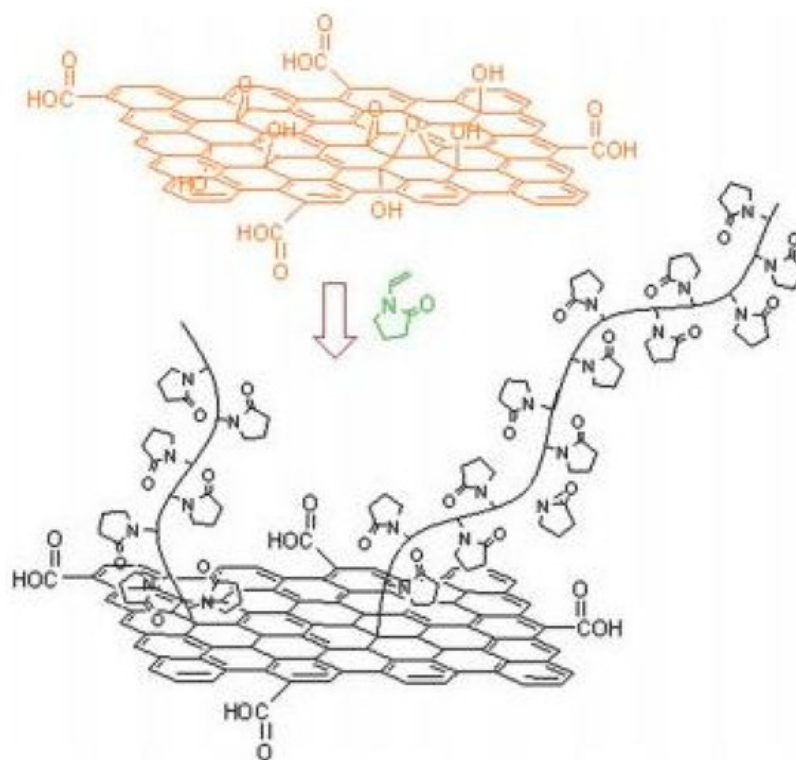


**Figure 3.** GO surface-initiated polymerization of N-vinylpyrrolidone [19].

## 2.4. UCNPs and Hybrid QPIs

Upconverting nanoparticles (UCNPs) are luminescent materials that are capable of emitting higher energy, lower wavelength photons on absorption of lower energy, higher wavelength incident light [24][25][26][27][28][29][30][31][32][33][34]. This photophysical phenomenon, which is referred to as photon upconversion, is based on an anti-Stokes process and involves sequential absorption of two or more low-energy photons, which enables the population of real, intermediate excited electronic states, followed by emission of a single high-energy photon. The commonly studied UCNPs are based on a NaYF<sub>4</sub> crystalline host matrix, which includes activator (e.g., Er<sup>3+</sup> and Tm<sup>3+</sup>) lanthanide ions, as well as an upconversion sensitizer (e.g., Yb<sup>3+</sup>). The UCNPs showed anti-Stokes shifted visible, as well as ultraviolet, emission with a minimal autofluorescence background after excitation of the UCNPs by near-infrared (NIR) continuous wave laser light [24][25][26][27][28][29][30]. Recently, a number of reports have suggested these UCNPs possess low quantum yields, and enhancement in up conversion luminescence can be effectively achieved by doping with plasmonic semiconductor nanocrystals (**Figure 4**). Liu et al. reviewed several strategies to increase up conversion luminescence efficiency, such as energy transfer modulation, surface passivation, host lattice manipulation, photonic crystal engineering, broadband

sensitization, and surface plasmonic coupling. Rationally designed nanohybrids of UCNPs with enhanced photocatalytic activity behave as effective panchromatic radical photoinitiators [31][32][33][34].

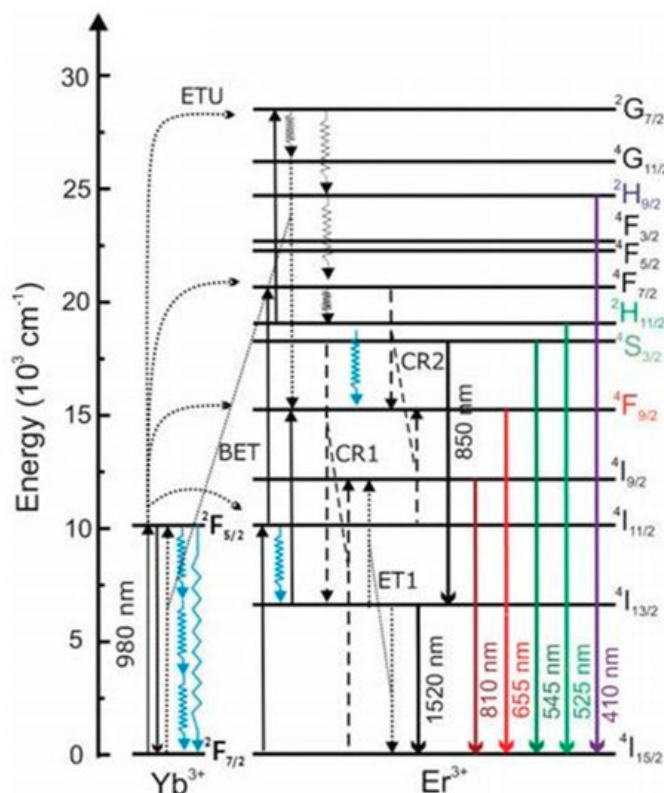


**Figure 4.** Energy scheme of Yb<sup>3+</sup>, Er<sup>3+</sup> co-doped NaYF<sub>4</sub>; ET: energy transfer, ETU: energy transfer upconversion, CR: cross relaxation, and BET: back energy transfer. The Yb<sup>3+</sup> ground state absorption (GSA) processes do not generally occur at the same Yb<sup>3+</sup> ion or at neighboring Yb<sup>3+</sup> ions, yet the absorbed energy migrates from the absorption site to Yb<sup>3+</sup> ions adjacent to Er<sup>3+</sup> upconverting centers. Thus, the Yb<sup>3+</sup> energy level diagram represents Yb<sup>3+</sup> in the NaYF<sub>4</sub> lattice, whereas the Er<sup>3+</sup> energy level diagram represents a single Er<sup>3+</sup> ion. Right, top panels: P-dependence of the photon upconversion luminescence of DSPE-stabilized UCNPs in water and D<sub>2</sub>O. Exemplarily shown are spectrally corrected emission spectra of DSPE-capped UCNPs in water (black lines) and D<sub>2</sub>O (red lines) at low P of ca. 16 W cm<sup>-2</sup> [40].

## 2.5. Polymer-Hybrid QPIs

Generally, organic compounds are used as Type I and II photoinitiators in UV-Vis curing technology for the fabrication of functional polymeric materials, including inks, coatings, and adhesives. Type I photoinitiators are known to undergo  $\alpha$ -cleavage and decompose into two radical species under UV-Vis light irradiation [41] and type II photoinitiators form radicals via a multi-step reaction process in the presence of co-initiators. Amines are commonly used as a co-initiator; an electron is transferred to the triplet state in the type II initiator, resulting in proton release to form radicals. Commercially available type II initiators with broad wavelength absorption over UV-Vis wavelengths include thioxanthone (TX) and its derivatives, benzophenone (BP) and camphorquinone (CQ). However, these compounds are relatively small in size and can enter the polymer matrix while cross linking. Thus, the small molecular type I photoinitiators are often attached to polymeric nanoparticles to produce efficient photoinitiator systems [41].

Du et al. demonstrated an strategy involving the combination of a type I photoinitiator and the nanoparticles of a functionalized block copolymer through reversible addition-fragmentation chain transfer (RAFT)-mediated polymerization-induced self-assembly (PISA) in an aqueous medium; the choice of the block copolymer nanoparticle affects the properties of the hydrogel that is prepared (Figure 5). Using this approach, hydrogels with embedded nanoparticles may be prepared using block copolymer nanoparticle-based heterogeneous photoinitiators [41].



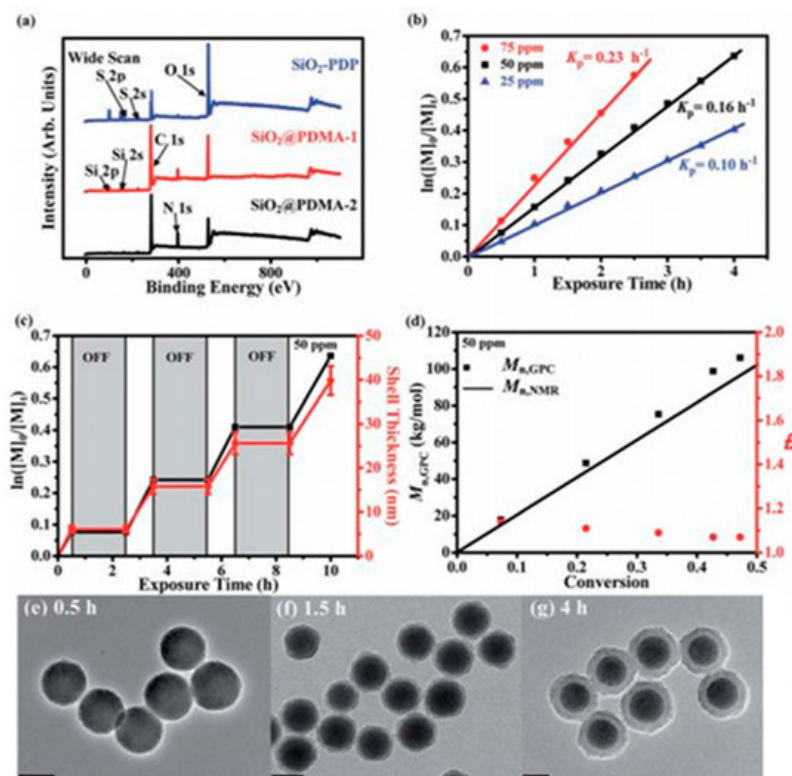


**Figure 5.** Surface-initiated PET-RAFT polymerization of DMA monomers from SiO<sub>2</sub>-PDP nanoparticles in acetonitrile with prior deoxygenation at 25 °C under blue LED light irradiation (4.8 W,  $\lambda$  max  $\frac{1}{4}$  465 nm, 1.0 mW cm<sup>2</sup>). (a) XPS wide-scan spectra of SiO<sub>2</sub>-PDP, SiO<sub>2</sub>@PDMA-1, and SiO<sub>2</sub>@PDMA-2 nanoparticles; (b) plot of  $\ln([M]_0/[M]_t)$  versus exposure time  $t$  at three different Ru(bpy)<sub>3</sub>Cl<sub>2</sub> concentrations with reference to monomer concentration; (c) temporal control over polymerization upon on/off switching of light; and (d) evolution of  $M_n$ ,NMR,  $M_n$ ,GPC, and  $\bar{D}$  versus monomer conversion. TEM images of (e) SiO<sub>2</sub>@PDMA-1, (f) SiO<sub>2</sub>@PDMA-2, and (g) SiO<sub>2</sub>@PDMA-3 nanoparticles. All scale bars are 100 nm [42].

Li et al. described polymer brush growth from the surface of silica nanomaterials via the PET-RAFT approach [42]. Through spatiotemporal control over light regulation, silica nanocomposites that were coated by polymer brushes with narrow molecular weight dispersities and high grafting densities were prepared; for example, surface-initiated polymerization of DMA monomers from SiO<sub>2</sub>-PDP nanoparticles under blue LED light irradiation using the PET-RAFT approach was demonstrated (Figure 6) [42].

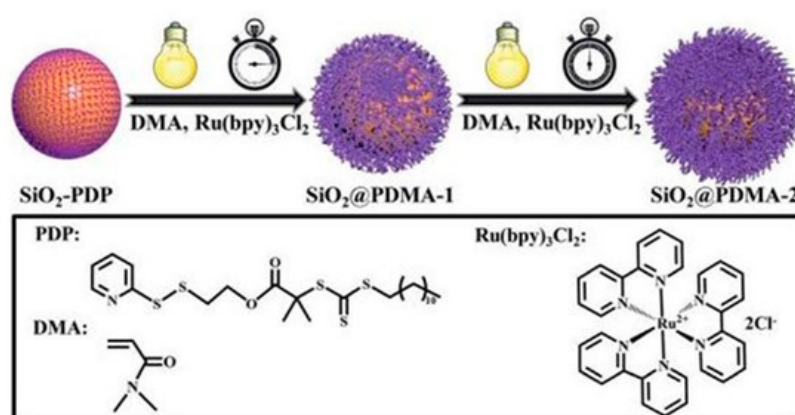


**Figure 6.** Surface-initiated PET-RAFT polymerization of DMA monomers from SiO<sub>2</sub>-PDP nanoparticles in acetonitrile, with prior deoxygenation at 25 °C under blue LED light irradiation [42].

## References

1. Waiskopf, N.; Ben-Shahar, Y.; Banin, U. Photocatalytic hybrid semiconductor–metal nanoparticles; from synergistic properties to emerging applications. *Adv. Mater.* 2018, 30, 1706697.

2. Schmitt, M. ZnO Nanoparticle Induced Photo-Kolbe Reaction, Fragment Stabilization and Effect on Photopolymerization Monitored by Raman–UV-Vis Measurements. *Macromol. Chem. Phys.* 2012, 213, 1953–1962.
3. Schmitt, M.; Lalevée, J. ZnO nanoparticles as polymerisation Photo-Initiator: Levulinic acid/NaOH content variation. *Colloids Surf. A Physicochem. Eng. Asp.* 2017, 532, 189–194.
4. Ojah, R.; Dolui, S.K. Solar radiation-induced polymerization of methyl methacrylate in the presence of semiconductor-based photocatalyst. *Sol. Energy. Mater. Sol. Cells* 2006, 90, 1615–1620.
5. Strandwitz, N.C.; Khan, A.; Boettcher, S.W.; Mikhailovsky, A.A.; Hawker, C.J.; Nguyen, T.Q.; Stucky, G.D. One-and two-photon induced polymerization of methylmethacrylate using colloidal CdS semiconductor quantum dots. *J. Am. Chem. Soc.* 2008, 130, 8280–8288.
6. Zhang, D.; Yang, J.; Bao, S.; Wu, Q.; Wang, Q. Semiconductor nanoparticle-based hydrogels prepared via self-initiated polymerization under sunlight, even visible light. *Sci. Rep.* 2013, 3, 1–7.
7. Verbitsky, L.; Waiskopf, N.; Magdassi, S.; Banin, U. A clear solution: Semiconductor nanocrystals as photoinitiators in solvent free polymerization. *Nanoscale* 2019, 11, 11209–11216.
8. Kuriacose, J.C.; Markham, M.C. Mechanism of the Photo-Initiated Polymerization of Methyl Methacrylate at Zinc Oxide Surfaces. *J. Phys. Chem.* 1961, 65, 2232–2236.
9. Waiskopf, N.; Magdassi, S.; Banin, U. Quantum Photoinitiators: Toward Emerging Photocuring Applications. *J. Am. Chem. Soc.* 2021, 143, 577–587.
10. Pinkas, A.; Waiskopf, N.; Gigi, S.; Naor, T.; Layani, A.; Banin, U. Morphology Effect on Zinc Oxide Quantum Photoinitiators for Radical Polymerization. *Nanoscale* 2021, 3, 7152–7160.
11. Zhou, J.; Allonas, X.; Ibrahim, A.; Liu, X. Progress in the development of polymeric and multifunctional photoinitiators. *Prog. Polym. Sci.* 2019, 99, 101165.
12. Feng, J.; Ye, D. Polymerizable ZnO photoinitiators of surface modification with hydroxyl acrylates and photopolymerization with UV-curable waterborne polyurethane acrylates. *Eur. Polym. J.* 2019, 120, 109252.
13. Dadashi-Silab, S.; Atilla Tasdelen, M.; Mohamed Asiri, A.; Bahadar Khan, S.; Yagci, Y. Photoinduced atom transfer radical polymerization using semiconductor nanoparticles. *Macromol. Rapid Comm.* 2014, 35, 454–459.
14. Huang, Y.; Zhu, Y.; Egap, E. Semiconductor quantum dots as photocatalysts for controlled light-mediated radical polymerization. *ACS Macro Lett.* 2018, 7, 184–189.
15. Liang, E.; Liu, M.S.; He, B.; Wang, G.X. ZnO as photocatalyst for photoinduced electron transfer–reversible addition–fragmentation chain transfer of methyl methacrylate. *Adv. Polym. Technol.* 2018, 37, 2879–2884.
16. Liao, J.; Ye, D. Improving ZnO photoinitiation efficiency by surface reaction with 2-hydroxy-2-methylpropiophenone. *Eur. Polym. J.* 2021, 147, 110293.
17. Han, Y.; Wang, F.; Lim, C.Y.; Chi, H.; Chen, D.; Wang, F.; Jiao, X. High-performance nano-photoinitiators with improved safety for 3D printing. *ACS Appl. Mater. Interfaces.* 2017, 9, 32418–32423.
18. Huang, Y.; Zeng, M.; Ren, J.; Wang, J.; Fan, L.; Xu, Q. Preparation and swelling properties of graphene oxide/poly (acrylic acid-co-acrylamide) super-absorbent hydrogel nanocomposites. *Colloids Surf. A Physicochem. Eng. Asp.* 2012, 401, 97–106.
19. Feng, R.; Zhou, W.; Guan, G.; Li, C.; Zhang, D.; Xiao, Y.; Zheng, L.; Zhu, W. Surface decoration of graphene by grafting polymerization using graphene oxide as the initiator. *J. Mater. Chem.* 2012, 22, 3982–3989.
20. Andryushina, N.S.; Stroyuk, O.L.; Dudarenko, G.V.; Kuchmiy, S.Y.; Pokhodenko, V.D. Photopolymerization of acrylamide induced by colloidal graphene oxide. *J. Photochem. Photobiol. A* 2013, 256, 1–6.
21. Feng, Y.; Peng, C.; Li, Y.; Hu, J.; Deng, Q.; Wu, Q.; Xu, Z. Superhydrophobic nanocomposite coatings with photoinitiated three-dimensional networks based on reactive graphene nanosheet-induced self-wrinkling patterned surfaces. *J. Colloid. Interface. Sci.* 2019, 536, 149–159.
22. Sangermano, M.; Marchi, S.; Valentini, L.; Bon, S.B.; Fabbri, P. Transparent and conductive graphene oxide/poly (ethylene glycol) diacrylate coatings obtained by photopolymerization. *Macromol. Mater. Eng.* 2011, 296, 401–407.
23. Wang, X.; Xing, W.; Song, L.; Yu, B.; Hu, Y.; Yeoh, G.H. Preparation of UV-curable functionalized graphene/polyurethane acrylate nanocomposite with enhanced thermal and mechanical behaviors. *React. Funct. Polym.* 2013, 73, 854–858.
24. Chen, Z.; Oprych, D.; Xie, C.; Kutahya, C.; Wu, S.; Strehmel, B. Upconversion-nanoparticle-assisted radical polymerization at  $\lambda = 974$  nm and the generation of acidic cations. *ChemPhotoChem* 2017, 1, 499–503.

25. Li, Z.; Chen, H.; Wang, C.; Chen, L.; Liu, J.; Liu, R. Efficient photopolymerization of thick pigmented systems using upconversion nanoparticles-assisted photochemistry. *J. Polym. Sci. A Polym. Chem.* 2018, 56, 994–1002.
26. Rocheva, V.V.; Koroleva, A.V.; Savelyev, A.G.; Khaydukov, K.V.; Generalova, A.N.; Nechaev, A.V.; Guller, A.E.; Semchishen, V.A.; Chichkov, B.N.; Khaydukov, E.V. High-resolution 3D photopolymerization assisted by upconversion nanoparticles for rapid prototyping applications. *Sci. Rep.* 2018, 8, 1–10.
27. Qin, X.; Carneiro Neto, A.N.; Longo, R.L.; Wu, Y.; Malta, O.L.; Liu, X. Surface Plasmon–Photon Coupling in Lanthanide-Doped Nanoparticles. *J. Phys. Chem. Lett.* 2021, 12, 1520–1541.
28. Wang, K.; Peña, J.; Xing, J. Upconversion Nanoparticle-Assisted Photopolymerization. *Photochem. Photobiol.* 2020, 96, 741–749.
29. Bagheri, A.; Arandiyani, H.; Adnan, N.N.M.; Boyer, C.; Lim, M. Controlled direct growth of polymer shell on upconversion nanoparticle surface via visible light regulated polymerization. *Macromolecules* 2017, 50, 7137–7147.
30. Oprych, D.; Schmitz, C.; Ley, C.; Allonas, X.; Ermilov, E.; Erdmann, R.; Strehmel, B. Photophysics of Up-Conversion Nanoparticles: Radical Photopolymerization of Multifunctional Methacrylates Comprising Blue-and UV-Sensitive Photoinitiators. *ChemPhotoChem* 2019, 3, 1119–1126.
31. Zhang, J.; Huang, Y.; Jin, X.; Nazartchouk, A.; Liu, M.; Tong, X.; Jiang, Y.; Ni, L.; Sun, S.; Sang, Y.; et al. Plasmon enhanced upconverting [email protected] triple-shell nanoparticles as recyclable panchromatic initiators (blue to infrared) for radical polymerization. *Nanoscale Horiz.* 2019, 4, 907–917.
32. Jee, H.; Chen, G.; Prasad, P.N.; Ohulchanskyy, T.Y.; Lee, J. In Situ Ultraviolet Polymerization Using Upconversion Nanoparticles: Nanocomposite Structures Patterned by Near Infrared Light. *Nanomaterials* 2020, 10, 2054.
33. Ding, C.; Wang, J.; Zhang, W.; Pan, X.; Zhang, Z.; Zhang, W.; Zhu, J.; Zhu, X. Platform of near-infrared light-induced reversible deactivation radical polymerization: Upconversion nanoparticles as internal light sources. *Polym. Chem.* 2016, 7, 7370–7374.
34. Hu, L.; Hao, Q.; Wang, L.; Cui, Z.; Fu, P.; Liu, M.; Qiao, X.; Pang, X. The in situ “grafting from” approach for the synthesis of polymer brushes on upconversion nanoparticles via NIR-mediated RAFT polymerization. *Polym. Chem.* 2021, 12, 545–553.
35. Nehlig, E.; Schneider, R.; Vidal, L.; Clavier, G.; Balan, L. Silver nanoparticles coated with thioxanthone derivative as hybrid photoinitiating systems for free radical polymerization. *Langmuir* 2012, 28, 17795–17802.
36. Yang, Y.; Zhao, Y.; Yan, Y.; Wang, Y.; Guo, C.; Zhang, J. Preparation of AgCl nanocubes and their application as efficient photoinitiators in the polymerization of N-isopropylacrylamide. *J. Phys. Chem. B* 2015, 119, 14807–14813.
37. Kiskan, B.; Zhang, J.; Wang, X.; Antonietti, M.; Yagci, Y. Mesoporous graphitic carbon nitride as a heterogeneous visible light photoinitiator for radical polymerization. *ACS Macro Lett.* 2012, 1, 546–549.
38. Dadashi-Silab, S.; Tasdelen, M.A.; Kiskan, B.; Wang, X.; Antonietti, M.; Yagci, Y. Photochemically mediated atom transfer radical polymerization using polymeric semiconductor mesoporous graphitic carbon nitride. *Macromol. Chem. Phys.* 2014, 215, 675–681.
39. Fu, Q.; Ruan, Q.; McKenzie, T.G.; Reyhani, A.; Tang, J.; Qiao, G.G. Development of a robust PET-RAFT polymerization using graphitic carbon nitride (g-C<sub>3</sub>N<sub>4</sub>). *Macromolecules* 2017, 50, 7509–7516.
40. Würth, C.; Kaiser, M.; Wilhelm, S.; Grauel, B.; Hirsch, T.; Resch-Genger, U. Excitation power dependent population pathways and absolute quantum yields of upconversion nanoparticles in different solvents. *Nanoscale* 2017, 9, 4283–4294.
41. Du, Y.; Jia, S.; Chen, Y.; Zhang, L.; Tan, J. Type I Photoinitiator-Functionalized Block Copolymer Nanoparticles Prepared by RAFT-Mediated Polymerization-Induced Self-Assembly. *ACS Macro Lett.* 2021, 10, 297–306.
42. Li, X.; Ye, S.; Huang, Y.; Le Li, J.; Cai, T. Precise growth of polymer brushes on silica-based nanocomposites via visible-light-regulated controlled radical polymerization. *J. Mater. Chem. A* 2019, 7, 6173–6179.